

Classification of continuous order-disorder transitions in adsorbed monolayers. II

E. Domany and M. Schick

Department of Physics, University of Washington, Seattle, Washington 98195

(Received 25 May 1979)

We extend the classification of continuous order-disorder transitions in adsorbed systems to encompass additional situations of physical interest. Among these are transitions on substrate arrays which are not simple Bravais lattices. The honeycomb and kagomé lattices are treated in detail. Their transitions belong to the universality class of the Ising, three- or four-state Potts model, and the Heisenberg model with cubic anisotropy. A simple case of the transitions of diatomic molecules is also considered. Those of Br₂ on graphite are predicted to be first order. Lastly, transitions between ordered states are analyzed and an example of experimental interest is discussed.

I. INTRODUCTION

Structural order-disorder transitions in adsorbed monolayers are of considerable theoretical and experimental interest.¹⁻¹¹ In a recent publication¹¹ (referred to as I) a classification of the continuous order-disorder transitions of simple adsorbed systems which was based upon the Landau theory was presented. In this paper we extend the preceding work to encompass additional experimentally relevant situations whose analysis is somewhat more complex. In particular whereas the analysis in I was restricted to cases in which there is one adsorption site per unit cell we consider here the honeycomb and kagomé lattices with, respectively, two and three adsorption sites per unit cell of the triangular Bravais lattice. Physical realizations of both lattices are considered in Sec. II. In addition, where I treated the adsorption of structureless atoms, we also consider the adsorption of molecules. The simple case of a diatomic homonuclear molecule like Br₂ is addressed. Lastly, where previously only transitions from the disordered phase were considered, we analyze here transitions between two ordered phases. An experimentally relevant example is considered. In all cases, we continue to limit ourselves to commensurate structures characterized by a \vec{k} vector that does not vary with temperature and coverage.

Our analysis, presented in Sec. III is based, as before, on symmetry considerations of Landau and Lifshitz.¹² For a discussion of the underlying theory and applicability to two dimensions, the interested reader is referred to previous work.¹¹⁻¹³ Our results are summarized in Sec. IV. For the honeycomb and kagomé lattices we find that the allowed continuous transitions belong to the universality classes of the two-dimensional Ising, three- or four-state Potts models, and Heisenberg model with cubic anisotropy.

II. REALIZATION OF HONEYCOMB AND KAGOMÉ LATTICES

A honeycomb array of adsorption sites is easily prepared for both chemisorbed and physisorbed systems. For the former it is usually sufficient to cleave an fcc or bcc crystal along the (111) face in which the substrate atoms are in a close-packed triangular array. If, as in many cases, the preferred adsorption sites are at the points of threefold symmetry, then the array of such sites forms a honeycomb lattice. Chemisorbed systems have the advantage of displaying an extremely rich variety of order-disorder transitions which are easily monitored by low-energy electron-diffraction techniques. Unfortunately they are not, at present, suitable for the determination of critical exponents. This is due to the high transition temperatures and small surface to volume ratios which do not permit direct measurements of the specific heat and the exponent α , and the limited coherence of the electron beam which prevents an accurate determination of the onset of order and the exponent β . Improved techniques or alternate ones, such as the use of a strain gauge¹⁴ which is sensitive to α , may make feasible the measurement of critical exponents in chemisorbed systems.

In physisorbed systems, a honeycomb lattice of adsorption sites is again provided by a substrate whose atoms are in a close-packed triangular array. This array can occur naturally, as in the laminar halides,¹⁵ or be brought about by preplating another substrate, like graphite, with a noble gas of high heat of adsorption.¹⁶ The preplated system then provides the desired array for a more weakly bound substance, such as He. While physisorbed systems do not display the diversity of order-disorder transitions manifested by chemisorbed systems, they possess the advantage that both α and β can be measured.

Values of each for one transition have so far been reported.^{3,4}

One important difference between the honeycomb array presented by the preplated systems and those presented by the laminar halides or (111) crystal faces is that in the former all adsorption sites are equivalent. The space group is $p6mm$. In the latter the degeneracy in the energy of adsorption is lifted by layers of substrate atoms below the surface. The result is that the honeycomb array with nearest-neighbor distance a decomposes into two triangular sublattices of lattice spacing $\sqrt{3}a$. The sites on one sublattice are not equivalent to those on the other so that the symmetry is reduced to $p3m1$.

Whereas a honeycomb lattice results from adsorption at the threefold symmetric sites presented by the close-packed array of substrate atoms, a kagomé lattice of sites results if adsorption occurs at the "bridge sites" midway between pairs of substrate atoms. This is not a very common site for the adsorption of single atoms. However, a physical realization of the kagomé lattice is provided by the physisorption of a diatomic molecule, like Br_2 , on graphite.¹⁷ Because the distance between the two Br atoms is quite close to that between the nearest-neighbor adsorption sites of graphite, the lowest state of an adsorbed molecule is that shown in Fig. 1 in which the molecule is lying down.¹⁸ The statistical mechanics of such a system can be discussed employing a triangular lattice-gas model with the constraint that if any site is occupied

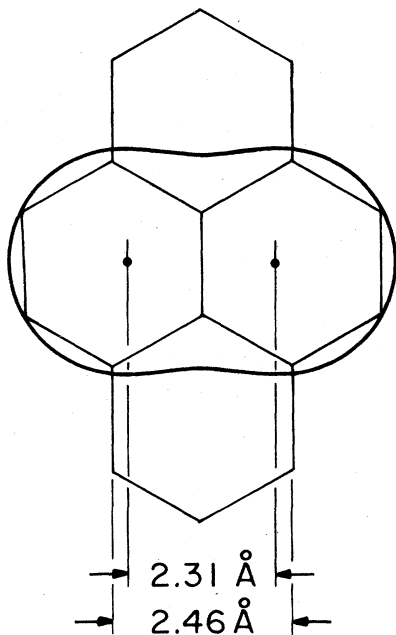


FIG. 1. Br_2 molecule adsorbed on the basal plane of graphite. The distance between two Br atoms (2.31 \AA) is close to that between two nearest adsorption sites (2.46 \AA).

at least one nearest-neighbor site is also occupied. Alternatively one can note that the position of a Br_2 molecule adsorbed as shown in Fig. 1 can be specified entirely by the position of its center of mass which will always fall at a "bridge" site. Thus the problem can also be treated as a kagomé lattice gas with fairly complicated interactions between molecules. Since the Landau-type analysis depends only on the symmetry of the Hamiltonian and not on the form of the interactions, one can use the results of such an analysis of the kagomé lattice to discuss continuous transitions for the Br_2 on graphite system.

III. SYMMETRY ANALYSIS

In this section we present a brief review of the method that was discussed in detail in I and then turn to applications to the honeycomb and kagomé lattices and to transitions between ordered structures.

We consider a lattice of identical adsorption sites with position vectors \vec{r} . Each site is either occupied [$n(\vec{r}) = 1$] or empty [$n(\vec{r}) = 0$]. Any configuration $\{n(\vec{r})\}$ will appear with the statistical weight given by $\exp[-(H\{n\} - \mu N)/kT]$ where $N = \sum_{\vec{r}} n(\vec{r})$ and $H\{n\}$ contains two, three, ..., etc., particle interactions. In the high-temperature phase the density $\rho(\vec{r})$ which is equal to the ensemble average $\langle n(\vec{r}) \rangle$ takes the value ρ_0 independent of \vec{r} . Thus the function $\rho(\vec{r})$ has the symmetry G_0 of the lattice of adsorption sites ($p6mm$ for the kagomé lattice, $p6mm$ or $p3m1$ for the honeycomb). In the ordered phase the density is no longer uniform and can be written

$$\rho(\vec{r}) = \rho_0 + \delta\rho(\vec{r}) ,$$

where

$$\delta\rho(\vec{r}) = \sum_l' \sum_i C_{li} \Phi_{li}(\vec{r}) . \quad (1)$$

The index l sums over irreducible representations of G_0 , and i over functions within a representation. The prime denotes exclusion of the unit representation.

We utilize the phenomenological Landau-Lifshitz¹² theory of continuous phase transitions in order to construct the Landau-Ginzburg-Wilson (LGW) Hamiltonian that corresponds to the transition to an ordered state. If the LGW Hamiltonian is that of a known model, we identify the universality class of the transition with that of the known model. Of the infinite variety of possible ordered superlattice structures we limit our attention to a finite class. First we consider only those cases in which $\delta\rho(\vec{r})$ belongs to a single irreducible representation of G_0 , the leading representation. We denote this representation by T . The ordered state is characterized by a nonvanishing expectation value of the order parameter

$$\psi_{T,i} \equiv \sum_{\vec{r}} \Phi_{T,i}(\vec{r}) n(\vec{r}) , \quad (2)$$

where i labels the components of ψ which are equal in number to the dimensionality of T . However, the occurrence of a nonzero contribution to $\delta\rho(\vec{r})$ from T can indirectly induce contributions from other representations due to invariants in the free energy which couple the two representations. Examples of this coupling mechanism are given in I. When such terms are involved in the specifications of $\delta\rho(\vec{r})$ of physically interesting ordered states, we shall note them.

We further limit our attention to transitions to simple commensurate structures characterized by a fixed \vec{k} . The value of the characteristic \vec{k} vector can be fixed by two mechanisms. First, if the Lifshitz condition is satisfied, (i.e., the antisymmetric part of T^2 does not contain the vector representation) the LGW Hamiltonian will contain no terms that are linear in \vec{k} and quadratic in the order parameter. Thus there will be a minimum at the characteristic \vec{k} . When the Lifshitz condition is not satisfied, \vec{k} can still be fixed at a commensurate value by some term in the LGW Hamiltonian which is of higher than second order in the components of the order parameter (umklapp term). In such a case, mean-field theory predicts a first-order transition to the ordered structure. In two dimensions, however, we know that transitions driven by such higher-order terms can be continuous (e.g., the three- and four-state Potts models). Therefore predictions based on the Lifshitz rule concerning the order of the transition must be checked experimentally and by independent theoretical models. Here we consider only those representations characterized by a wave vector at which the Lifshitz condition can be satisfied. These wave vectors belong to one of the irreducible stars of Fig. 2, namely $\vec{k}=0$, or \vec{q}_1, \vec{q}_2 or $\vec{k}_1, \vec{k}_2, \vec{k}_3$.

The basis functions Φ of Eqs. (1) and (2) take different forms depending on whether the array of adsorption sites is a simple Bravais lattice, as in I, or is not. For clarity we denote the position vectors of the adsorption sites by \vec{r} and that of the Bravais lattice points by \vec{R} . In the case considered in I, $\vec{r}=\vec{R}$ and

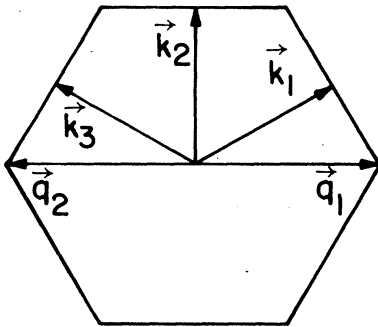


FIG. 2. \vec{k} vectors that characterize the superlattice structures considered in this paper.

the functions Φ can be written (we drop the subscript T) $\Phi_i(\vec{R}) = \phi_{\vec{k}_i}(\vec{R})$ where $\phi_{\vec{k}_i}(\vec{R})$ is either $\sin \vec{k}_i \cdot \vec{R}$ or $\cos \vec{k}_i \cdot \vec{R}$. There are m independent functions $\phi_{\vec{k}_i}(\vec{R})$ equal to the number of independent vectors \vec{k}_i in the star of \vec{k} . When the lattice of adsorption sites is a Bravais lattice plus a basis of more than one site per unit cell, the position of a site \vec{r} is obtained by assigning each site uniquely to a unit cell specified by \vec{R} and introducing the position vector \vec{X} of the site with respect to the origin of the unit cell. Then $\vec{r}=\vec{R}+\vec{X}$ and the functions Φ can be written in the product form

$$\Phi_{j,\alpha}(\vec{r}) = \phi_{\vec{k}_j}(\vec{R}) W_\alpha(\vec{X}) \quad (3)$$

(\vec{r} unique) where the $W_\alpha(\vec{X})$ provide a basis for the irreducible representations of the group of the \vec{k} vector, or small group. If the representation of the small group is l dimensional, there are lm independent functions $\Phi_j(\vec{r})$ and the same number of components of the order parameter.

We now specify the functions $W_\alpha(\vec{X})$. The number of independent $W_\alpha(\vec{X})$ is simply the number of sites per unit cell, two and three for the honeycomb and kagomé lattices, respectively. Rather than define two such functions for the honeycomb lattice and three other functions for the kagomé lattice, we define an overcomplete set of six functions which can be applied to either case. In particular, we choose as a unit cell the basic hexagon which occurs in either lattice. The center of any given hexagon is specified by the vector \vec{R} . The vector \vec{X} takes on six values \vec{X}_j as shown in Fig. 3(a) and specifies the six sites within the unit cell. Any given site belongs to three (two) different unit cells for the honeycomb (kagomé) lattice so that its position vector can be written in the same number of ways. For example the site shared by the three cells of Fig. 3(b) can be written $\vec{r}=\vec{R}_1+\vec{X}_1=\vec{R}_2+\vec{X}_5=\vec{R}_3+\vec{X}_3$. The product form for the functions Φ , given by Eq. (3) when \vec{r} is uniquely specified, is now generalized to

$$\Phi_{T,i}(\vec{r}) = \sum_{\vec{R}} \phi_{k_j}(\vec{R}) \sum_{\vec{X}} W_\alpha(\vec{X}) \delta_{\vec{r},\vec{R}+\vec{X}} \quad (4)$$

where $\delta_{\vec{r},\vec{r}'}$ is the Kronecker delta. With this form for the $\Phi_{T,i}$, Eq. (1) for the density variation becomes

$$\delta\rho(\vec{r}) = \sum_I C_{I,\alpha} \sum_{\vec{R}} \phi_{k_j}(\vec{R}) \sum_{\vec{X}} W_\alpha(\vec{X}) \delta_{\vec{r},\vec{R}+\vec{X}} \quad (5)$$

Like the ϕ_{k_j} , the functions $W_\alpha(\vec{X})$ can be chosen to be real. We choose the set

$$\begin{aligned} W_1(\vec{X}_1) &= 1, & W_2(\vec{X}_1) &= \cos(\frac{1}{3}\pi l), \\ W_3(\vec{X}_1) &= \sin(\frac{1}{3}\pi l), & W_4(\vec{X}_1) &= \cos(\frac{2}{3}\pi l), \\ W_5(\vec{X}_1) &= \sin(\frac{2}{3}\pi l), & W_6(\vec{X}_1) &= \cos(\pi l). \end{aligned}$$

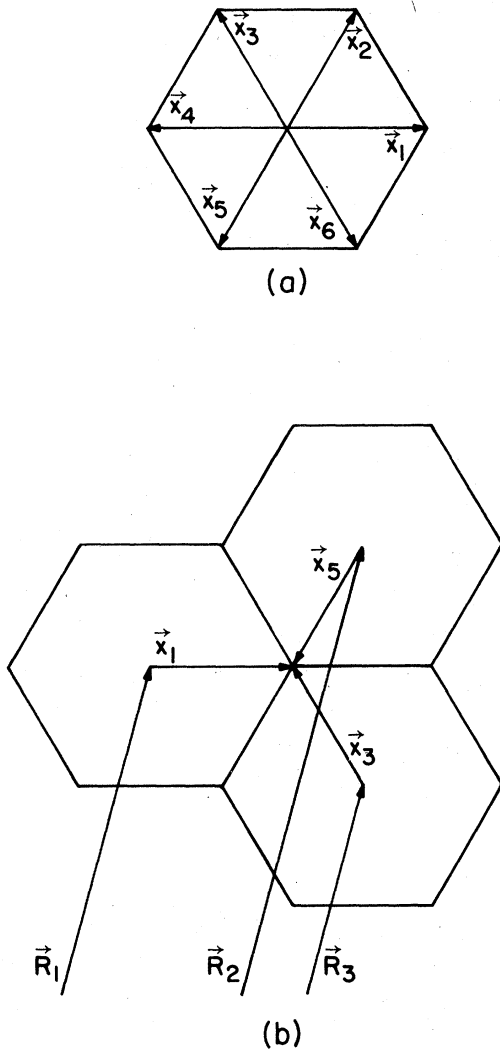


FIG. 3. Each adsorption site can be characterized by any one of the Bravais lattice sites closest to it, and an appropriate \vec{X}_j vector (a). The central site of the honeycomb array in (b) can be represented in three different such ways.

With a given representation now completely specified by the functions $\Phi_{T,i}(\vec{\tau})$, we can determine whether the representation satisfies the Lifshitz rule; that is whether the antisymmetric part of T^2 contains the vector representation, in which case the rule is violated, or does not contain it. The method of ascertaining this is straightforward.¹⁹ We note that it is easy to show that a representation characterized by one of the stars of Fig. 2 and a one-dimensional small representation satisfies the Lifshitz condition. Thus we will only remark on this condition when the small representation is of dimension greater than one.

We now apply this formalism to the honeycomb and kagomé lattices.

A. Honeycomb lattice

For each of the three stars of Fig. 2, $\vec{k}=0$, \vec{q}_1 , \vec{q}_2 , or \vec{k}_1 , \vec{k}_2 , \vec{k}_3 , we first consider the case in which all sites of the honeycomb lattice are equivalent and then the effect of the reduction of symmetry by a crystal field h_s of one sign on one triangular sublattice and of opposite sign on the other.

1. Case (i) $\vec{k}=0$

The small group is the entire point group C_{6v} . The function W_1 belongs to the unit representation. Its combination with $\vec{k}=0$ gives the unit representation of the entire lattice which is, by definition, excluded from Eq. (5) for $\delta\rho$. The function W_6 belongs to the one-dimensional representation B_1 and yields a density which corresponds to the structure of Fig. 4(a). The transition to this structure is Ising like. This density is thermodynamically conjugate to the crystal field h_s . Therefore in the physical circumstance in which h_s is nonzero, the Ising transition will be suppressed. All other W_α yield $\delta\rho(\vec{\tau})=0$ when substituted into Eq. (6).

2. Case (ii) \vec{q}_1, \vec{q}_2

The small group is C_{3v} . The two functions W_1 and W_6 belong to one-dimensional representations of C_{3v} but yield $\delta\rho(\vec{\tau})=0$ when substituted into Eq. (6). The functions W_2, W_3 belong to the two-dimensional representation E of the small group. Thus a four-

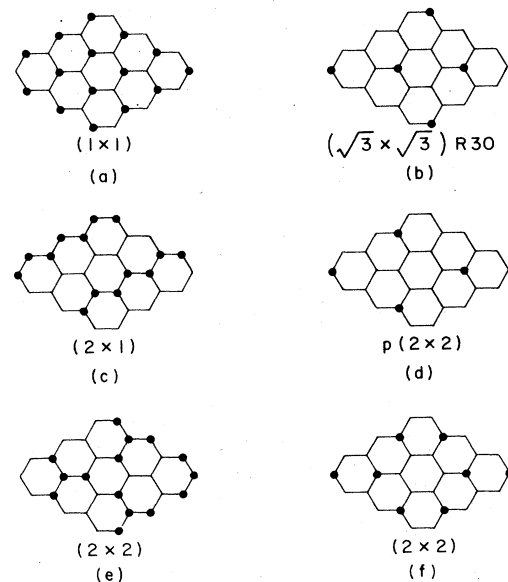


FIG. 4. "Physical" superlattice structures (allowing only integer occupation numbers) on the honeycomb array characterized by \vec{k} vectors of Fig. 2. See text for discussion of universality classes and order of the various transitions.

dimensional representation can be constructed. We define the basis functions

$$\begin{aligned}\Phi_1(\vec{r}) &= \sum_{\vec{R}, \vec{X}} [\cos(\vec{q}_1 \cdot \vec{R}) W_2(\vec{X}) \\ &\quad - \sin(\vec{q}_1 \cdot \vec{R}) W_3(\vec{X})] \delta_{\vec{R}+\vec{X}, \vec{r}} , \\ \Phi_2(\vec{r}) &= \sum_{\vec{R}, \vec{X}} [\cos(\vec{q}_1 \cdot \vec{R}) W_3(\vec{X}) \\ &\quad + \sin(\vec{q}_1 \cdot \vec{R}) W_2(\vec{X})] \delta_{\vec{R}+\vec{X}, \vec{r}} , \\ \Phi_3(\vec{r}) &= \sum_{\vec{R}, \vec{X}} [\cos(\vec{q}_1 \cdot \vec{R}) W_2(\vec{X}) \\ &\quad + \sin(\vec{q}_1 \cdot \vec{R}) W_3(\vec{X})] \delta_{\vec{R}+\vec{X}, \vec{r}} , \\ \Phi_4(\vec{r}) &= \sum_{\vec{R}, \vec{X}} [\cos(\vec{q}_1 \cdot \vec{R}) W_3(\vec{X}) \\ &\quad - \sin(\vec{q}_1 \cdot \vec{R}) W_2(\vec{X})] \delta_{\vec{R}+\vec{X}, \vec{r}} .\end{aligned}$$

The LGW Hamiltonian is

$$\begin{aligned}H &= r \sum_i \Phi_i^2 + u [\Phi_1^3 - 3\Phi_1\Phi_2^2 - (\Phi_3^3 - 3\Phi_3\Phi_4^2)] \\ &\quad + V[(\Phi_1^2 + \Phi_2^2)^2 + (\Phi_3^2 + \Phi_4^2)^2] \\ &\quad + W(\Phi_1^2 + \Phi_2^2)(\Phi_3^2 + \Phi_4^2) ,\end{aligned}\quad (6)$$

which can be seen to be that of two degenerate three-state Potts models which are coupled by the fourth-order term. By expressing the third-order invariant in terms of $\gamma_1 \equiv \frac{1}{2}(\Phi_1 + \Phi_3)$, $\gamma_2 \equiv \frac{1}{2}(\Phi_2 + \Phi_4)$, $\gamma_3 \equiv \frac{1}{2}(\Phi_2 - \Phi_4)$, and $\gamma_4 \equiv \frac{1}{2}(\Phi_3 - \Phi_1)$, we find that it is precisely that of a model discussed by Schick and Griffiths.²⁰ This four-dimensional representation does not satisfy the Lifshitz rule; i.e., we have verified that the antisymmetric part of T^2 does, in fact, contain the vector representation. According to the Lifshitz criterion then, a continuous transition is not expected. As noted earlier the reliability of such expectations is unclear. Therefore observation of a transition in this class would be quite interesting. There are several possible ordered states all of which are $\sqrt{3} \times \sqrt{3}$ $R30^\circ$ structures and correspond to coverages which are integer multiples of $\frac{1}{6}$. A simple example of coverage $\frac{1}{6}$ is shown in Fig. 4(b). The functions W_4, W_5 belong to the same two-dimensional representation of C_{3v} as W_2, W_3 and substitution into Eq.(6) shows that no new state is generated.

The effect of a crystal field is simply to lift the de-

generacy of the two three-state Potts models. Thus the one four-dimensional representation splits into two two-dimensional ones. One transition is expected which can be continuous and in the universality class of the three-state Potts model. Due to the coupling of the representations, the two components of the one representation which become nonzero at the transition can induce nonzero values of the components of the other representation. As a result several physical states are again possible. As above they are all characterized by simple $\sqrt{3} \times \sqrt{3}$ $R30^\circ$ structures on one or both triangular sublattices and correspond to coverages which are integer multiples of $\frac{1}{6}$. The example of coverage $\frac{1}{6}$ shown in Fig. 4(b) also applies.

We also stress that the transition to the above structures *can* be continuous. It *need not be*, particularly for small values of the field h_s . The reason is as follows. For vanishing h_s the fact that the Lifshitz condition is not satisfied indicates that the lowest-order terms in the LGW Hamiltonian do not produce a minimum at the values of $\vec{k} = \vec{q}_1$ or \vec{q}_2 . If a stable state characterized by these \vec{k} values is observed then it is stabilized by a higher-order term in the Hamiltonian. For small values of h_s this term will still dominate and if the transition for $h_s = 0$ is in fact first order, it will remain so. Only at sufficiently strong fields would a continuous transition be expected.

3. Case (iii) $\vec{k}_1, \vec{k}_2, \vec{k}_3$

The small group of \vec{k} is C_{2v} which has only one-dimensional irreducible representations. The functions W_1 and W_4 belong to the unit representation A_1 , W_2 and W_6 to the representation B_1 , and W_3 and W_5 to B_2 and A_2 , respectively. Use of W_1 or W_4 in Eqs. (4) and (5) generates the same three-dimensional representation which we can write

$$\Phi_{k_i,1}(\vec{r}) = \sum_{\vec{R}} \cos(\vec{k}_i \cdot \vec{R}) \sum_{\vec{X}} W_1(\vec{X}) \delta_{\vec{r}, \vec{R}+\vec{X}} .\quad (7)$$

The functions W_2 or W_6 generate another three-dimensional representation

$$\Phi_{k_i,2}(\vec{r}) = \sum_{\vec{R}} \cos(\vec{k}_i \cdot \vec{R}) \sum_{\vec{X}} W_2(\vec{X}) \delta_{\vec{r}, \vec{R}+\vec{X}} .\quad (8)$$

The LGW Hamiltonian can be written

$$\mathcal{H} = \mathcal{H}_{4p} + \mathcal{H}_H + \mathcal{H}_c ,\quad (9)$$

where

$$\mathcal{H}_{4p} = r_1 \sum_i \Phi_{k_i,1}^2 + u \Phi_{k_1,1} \Phi_{k_2,1} \Phi_{k_3,1} ,$$

$$\mathcal{H}_H = r_2 \sum_i \Phi_{k_i,2}^2 + V \left[\sum_i \Phi_{k_i,2}^2 \right]^2 + W \sum_i \Phi_{k_i,2}^4 ,$$

$$\begin{aligned}\mathcal{H}_c &= X(\Phi_{k_1,1} \Phi_{k_2,2} \Phi_{k_3,2} + \Phi_{k_1,2} \Phi_{k_2,1} \Phi_{k_3,2} + \Phi_{k_1,2} \Phi_{k_2,2} \Phi_{k_3,1}) + Y \phi_{0,6} \Phi_{k_1,2} \Phi_{k_2,2} \Phi_{k_3,2} \\ &\quad + Z \phi_{0,6} (\Phi_{k_1,1} \Phi_{k_2,1} \Phi_{k_3,2} + \Phi_{k_1,1} \Phi_{k_2,2} \Phi_{k_3,1} + \Phi_{k_1,2} \Phi_{k_2,1} \Phi_{k_3,1}) .\end{aligned}$$

The Hamiltonian \mathcal{H}_{4P} is that of a four-state Potts model, \mathcal{H}_H that of a Heisenberg model with cubic anisotropy and \mathcal{H}_c couples the two representations of Eqs. (7) and (8) and the one-dimensional $\vec{k}=0$ representation $\phi_{0,6}$. The combined Hamiltonian can describe a rich variety of behavior. Let us first assume that r_2 vanishes at a higher temperature than r_1 . In this case there can be a continuous transition in the class of the Heisenberg model with cubic anisotropy. The physical state realized depends on the sign of the anisotropy W . If W is positive then only one component of $\Phi_{k_i,2}$ will be nonzero and the physical 2×1 state of Fig. 4(c) will be attained. If W is negative, all components $\Phi_{k_i,2}$ will be nonzero and the coupling terms will induce nonzero values of $\Phi_{k_i,1}$ and $\phi_{0,6}$. The physical $p(2 \times 2)$ state of Fig. 4(d) can be reached in this way by a single continuous transition as can the unusual state of Fig. 4(e).

If r_1 vanishes at a higher temperature than r_2 then there can be a continuous transition in the class of the four-state Potts model. Due to the third-order invariant in \mathcal{H}_{4P} all $\Phi_{k_i,1}$ will be equal and nonzero just below the transition. The physical state is 2×2 shown in Fig. 4(f). Due to the nonzero values of $\Phi_{k_i,1}$ in the coupling Hamiltonian, the three-dimensional representation $\Phi_{k_i,2}$ reduces to a one-dimensional and a two-dimensional representation. If the one-dimensional representation becomes critical, an Ising transition can occur. The physical state reached is again the $p(2 \times 2)$ state of Fig. 4(d). Thus this state can be reached either by one Heisenberg transition or a four-state Potts transition followed by an Ising one. The two-dimensional representation does not lead to a physical state.

The above wealth of possibilities is for the case in which all honeycomb sites are equivalent. In the presence of a crystal field h_s the behavior is much simpler. To first order in h_s the LGW Hamiltonian is that of Eq. (9) with $\phi_{0,6}$ replaced by h_s in \mathcal{H}_c . As a result the Hamiltonian describes two nondegenerate coupled four-state Potts models. The physical states of Figs. 4(c)–4(f) can be reached by a single transition in the class of the four-state Potts model. Just below the transition, however, the state will look like that of Fig. 4(e) or 4(f) depending upon which representation becomes critical at a higher temperature. This is due to the third-order invariant which favors all three components of the representation being equal and results in these structures.

B. Kagomé lattice

1. Case (i) $\vec{k}=0$

The small group is C_{6v} . The function W_1 belongs to the unit representation and so, when combined

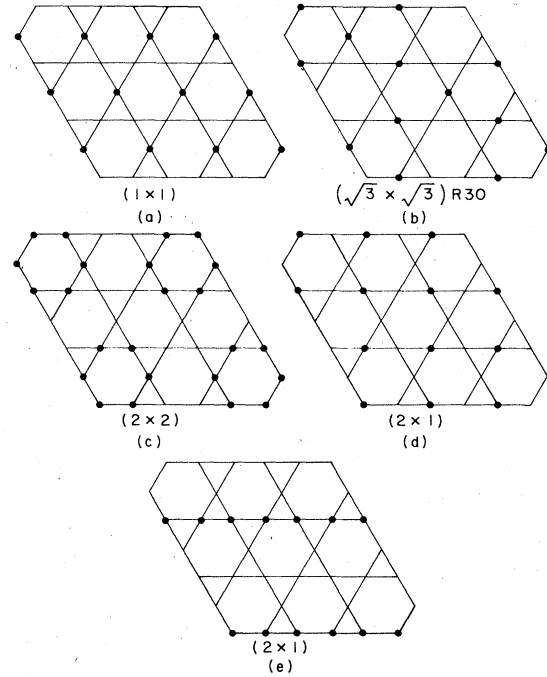


FIG. 5. "Physical" superlattice structures (allowing only integer occupation numbers) on the kagomé array characterized by \vec{k} vectors of Fig. 2. See text for discussion of universality class and order of the various transitions.

with $\vec{k}=0$ gives the unit representation of G_0 and is excluded. The three functions W_2 , W_3 , and W_6 lead to a vanishing density difference $\delta\rho(\vec{r})$. The two functions W_4 and W_5 belong to the two-dimensional representation E_2 . The Lifshitz condition is satisfied and the LGW Hamiltonian is that of the three-state Potts model. One of the three 1×1 structures is shown in Fig. 5(a).

2. Case (ii) \vec{q}_1, \vec{q}_2

The small group is C_{3v} . The two functions W_1 and W_6 which transform like the one-dimensional representations A_1 and A_2 yield identical structures. The LGW Hamiltonian is again that of the three-state Potts model. One of the three $\sqrt{3} \times \sqrt{3}$ $R30^\circ$ structures is shown in Fig. 5(b). The functions W_2 , W_3 belong to the two-dimensional representation E as do the functions W_4 , W_5 which give identical structures. The LGW Hamiltonian has an invariant like that of the model of Schick and Griffiths.²⁰ The Lifshitz condition is not satisfied for this representation.

3. Case (iii) $\vec{k}_1, \vec{k}_2, \vec{k}_3$

The small group is C_{2v} which, as noted earlier, has only one-dimensional representations. The functions W_1 , W_4 both transform like A_1 and give identical

structures and three-component order parameters. The LGW Hamiltonian contains a third-order invariant $\Phi_{k_1,1}\Phi_{k_2,1}\Phi_{k_3,1}$ and is that of the four-state Potts model. Just below the transition from the disordered phase all components of the order parameter are of equal magnitude and the structure is 2×2 shown in Fig. 5(c).

The function W_6 transforms like B_1 . The LGW Hamiltonian constructed from the three components of the order parameter contains no third-order terms as W_6 changes sign under some of the operations of G_0 . The Hamiltonian is that of the Heisenberg model with cubic anisotropy. When the sign of the anisotropy is negative favoring the nonvanishing of only one component of the order parameter, there are three 2×1 ordered structures of the form shown in Fig. 5(d). When the sign of the anisotropy is positive a complex 2×2 state is favored which can only be expressed by fractional occupation of the sites. Closely related to this representation is that generated by W_3 which transforms like B_2 . The LGW Hamiltonian is again that of the Heisenberg model with cubic anisotropy. For negative anisotropy there are three 2×1 states shown in Fig. 5(e) while a complex 2×2 state results from a positive anisotropy. All three of the above three-dimensional representations are coupled to the two-component $\vec{k}=0$ order parameter by terms of the form¹⁰

$$\Phi_{0,5}(\Phi_{k_2,1}^2 - \Phi_{k_3,1}^2) + 3^{-1/2}\Phi_{0,4}\left[3\Phi_{k_1,1}^2 - \sum_i \Phi_{k_i,1}^2\right].$$

Finally the functions W_2 and W_5 which transform like A_1 and A_2 , respectively, yield no new structures.

C. Order-order transitions

In this section we consider transitions from one ordered structure to another. As in Secs. III A and B, here also one has to deal with a Bravais lattice that has a basis. To be specific, we concentrate on a physical system of experimental relevance, oxygen chemisorbed on the (110) face of W.⁷ The adsorption sites form a centered rectangular lattice, and in the ordered state alternating diagonal rows are preferably occupied (see Fig. 6). Upon increase of coverage,

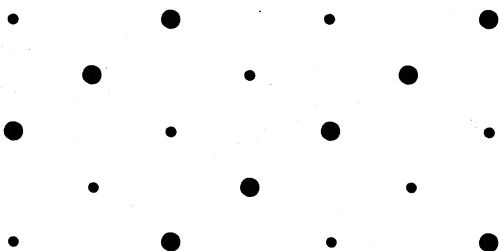


FIG. 6. Ordered state of oxygen on the (110) face of W, near atomic coverage of $\frac{1}{2}$.

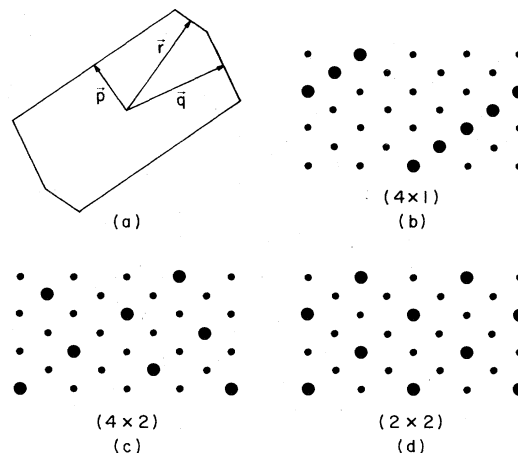


FIG. 7. Ordered states of lower symmetry, reached from the structure of Fig. 6. The structures characterized by the vectors p , q , and r of the Brillouin zone (a) are shown in (b), (c), and (d), respectively.

additional transitions may occur. To investigate these, the structure of Fig. 6 is considered as the high-symmetry phase, with symmetry group $P2$. Each unit cell contains two *nonequivalent* sites, one occupied with higher and the other with lower probability. The former will be designated as A sites, the latter as B sites. The A sites form the Bravais lattice. The group has only three representations that satisfy the Lifshitz condition, p , q , and r , corresponding to $\frac{1}{2}\bar{G}_1$, $\frac{1}{2}\bar{G}_2$, and $\frac{1}{2}(\bar{G}_1 + \bar{G}_2)$, where $\bar{G}_{1,2}$ are the reciprocal-lattice vectors. The Brillouin zone and the vectors p , q , r are shown in Fig. 7(a). The small group of all three is C_2 , which has only one-dimensional representations. These can be defined as

$$W_1(\vec{r}) = 1, \quad \text{for all } r,$$

$$W_2(\vec{r}) = \begin{cases} 1, & r \in A \\ -1, & r \in B \end{cases}.$$

Both functions belong to the unit representation of C_2 . For all three cases (p , q , or r) the transition is Ising like, and the physical states reached are shown in Fig. 7. With respect to the symmetry of the $W(110)$ surface, these states are 4×1 , 4×2 , and 2×2 . Note that the heavy dots may denote sites that are occupied with *lower* probability, corresponding to a "superlattice of vacancies."

IV. SUMMARY AND DISCUSSION

We have enumerated and classified the possible continuous transitions which can take place from disordered to commensurate ordered states on the honeycomb and kagomé lattices. In the former case it is necessary to distinguish those cases in which all adsorption sites are equally likely as in physisorption

on preplated graphite from those in which subsurface atoms provide a crystal field which decomposes the honeycomb lattice into two triangular lattices. In the case of preplated systems we find several possible transitions. An Ising transition is predicted to the ordered structure of Fig. 4(a). A physisorbed system which would undergo this transition would be of great interest to study because the expectation of a logarithmic specific heat is based upon several assumptions concerning, *inter alia*, the uniformity and effective dimensionality of these systems. Transitions to any $\sqrt{3} \times \sqrt{3}$ $R30^\circ$ structure such as that of Fig. 4(b) is predicted by the Lifshitz criterion to be first order. The validity of this criterion for commensurate transitions remains to be tested. The structures in Figs. 4(c)–4(e) can be reached by a continuous transition in the class of the Heisenberg model with cubic anisotropy. That of Fig. 4(f) can be reached by a transition in the class of the four-state Potts model. This class is certainly one of the most interesting theoretically.²¹ Further, its exponents are thought to be known²² and physisorbed systems which might undergo this transition have been suggested.⁹ An additional Ising transition from the state of Fig. 4(f) could produce that of Fig. 4(d).

For chemisorbed systems the results are somewhat simpler. The transition to the state of Fig. 4(a) is suppressed. Transitions to $\sqrt{3} \times \sqrt{3}$ $R30^\circ$ phases can be continuous and in the class of the three-state Potts model. For small crystal fields, however, they may be first order. A transition to the state shown in Fig. 4(b) has been reported²³ in I on Ag(111). The states of Figs. 4(c)–(f) can be reached by a single continuous transition in the class of the four-state Potts model. Continuous transitions to the state of Fig. 4(f)⁶ or Fig. 4(d)^{5,24} have been reported but no exponents have been measured.

For the kagomé lattice, continuous transitions are predicted to the structures of Fig. 5. The first two transitions are in the class of the three-state Potts model, the third in the class of the four-state Potts

model and the fourth and fifth in the class of the Heisenberg model with cubic anisotropy. An inspection of these figures and Fig. 1 reveals that none of these ordered structures can be obtained by the Br_2 molecule for all of them require occupancy of a given graphite absorption site by more than one Br atom. Therefore any ordered Br_2 structure must be characterized by a \bar{k} vector which does not satisfy the Lifshitz condition and hence the transition to this structure is predicted by mean-field theory to be first order. Again this needs to be tested. However we note that as the \bar{k} vector of any ordered Br_2 structure must belong to a star other than one shown in Fig. 2 it must contain at least six independent components which implies an order parameter with an equal number of components. This is the case of the 4×4 ordered structure suggested by Lander and Morrison.¹⁷ For Potts models, mean-field predictions of first-order transitions²⁵ become correct when the number of order-parameter components exceeds three. It appears plausible then that the prediction of first-order transitions for the Br_2 systems will also be correct.

Lastly we showed how the general methods could be applied to transitions from one ordered phase to another. We examined in particular the case of transitions from the 2×1 state of Fig. 6. We found that continuous Ising transitions were possible to the three structures of Fig. 7. The 2×2 structure of Fig. 7(d) is of interest because both it and the 2×2 structure of Fig. 6 have been observed in the system of O on W(110).⁷ Thus it should be possible to observe the transition between them.

ACKNOWLEDGMENT

Support from the NSF under Grants No. DMR 7721842 and No. DMR 7712676 A01 and a Dr. Ch. Weizmann Fellowship (E.D.) are gratefully acknowledged.

¹A guide to the literature on physisorption to 1974 is provided by J. G. Dash, *Films on Solid Surfaces* (Academic, New York, 1975). A convenient access to the chemisorption literature is provided by G. A. Somorjai, *Surf. Sci.* **34**, 156 (1973).
²M. Bretz, J. G. Dash, D. C. Hickernell, E. O. McLean, and O. E. Vilches, *Phys. Rev. A* **8**, 1589 (1973).
³M. Bretz, *Phys. Rev. Lett.* **38**, 501 (1977).
⁴P. M. Horn, R. J. Birgeneau, P. Heiney, and E. M. Hammonds, *Phys. Rev. Lett.* **41**, 961 (1978).
⁵A. R. Kortan, P. I. Cohen, and R. L. Park, *J. Vac. Sci. Technol.* (to be published).
⁶K. Christmann, R. J. Behm, G. Ertl, M. A. Van Hove, and W. H. Weinberg, *J. Chem. Phys.* **70**, 4168 (1979).
⁷J. C. Buchholtz and M. G. Lagally, *Phys. Rev. Lett.* **35**,

442 (1975).

⁸S. Alexander, *Phys. Lett. A* **54**, 353 (1975).

⁹E. Domany, M. Schick, and J. S. Walker, *Phys. Rev. Lett.* **38**, 1148 (1977).

¹⁰E. Domany and E. K. Riedel, *Phys. Rev. Lett.* **40**, 561 (1978).

¹¹E. Domany, M. Schick, J. S. Walker, and R. B. Griffiths, *Phys. Rev. B* **18**, 2209 (1978).

¹²L. D. Landau and E. M. Lifshitz, *Statistical Physics* (Addison-Wesley, Reading, Mass., 1969), Chap. XIII.

¹³D. Mukamel and S. Krinsky, *Phys. Rev. B* **13**, 5065 (1976).

¹⁴J. G. Dash, J. Suzanne, H. Shechter, and R. E. Peierls, *Surf. Sci.* **60**, 411 (1976).

¹⁵Y. Larher, *J. Colloid, Interface Sci.* **37**, 836 (1971).

- ¹⁶S. B. Crary and O. E. Vilches, Phys. Rev. Lett. 38, 973 (1977).
- ¹⁷J. J. Lander and J. Morrison, Surf. Sci. 6, 1 (1967).
- ¹⁸S. M. Heald and E. A. Stern, Phys. Rev. B 17, 4069 (1978).
- ¹⁹G. Ya. Lyubarskii, *The Application of Group Theory in Physics* (Pergamon, New York, 1960).
- ²⁰M. Schick and R. B. Griffiths, J. Phys. A 10, 2123 (1977).
- ²¹R. J. Baxter, J. Phys. C 6, L445 (1973).
- ²²Since the four-state Potts and the Baxter-Wu models lead to the same LGW Hamiltonian, the critical behavior of the two models is predicted to be the same. For the latter $\alpha = \frac{2}{3}$; R. J. Baxter and F. Y. Wu, Phys. Rev. Lett. 31, 1294 (1973).
- ²³F. Forstmann, W. Bernot, and P. Buttner, Phys. Rev. Lett. 30, 17 (1973).
- ²⁴A. U. MacRae, Surf. Sci. 1, 319 (1964).
- ²⁵J. P. Straley and M. E. Fisher, J. Phys. A 6, 1310 (1973).